

# SIMULATION OF FLUID FLOW IN WELD POOLS – A Review

**R. B. Choudary**

Assistant Professor, Department of Mechanical Engineering,  
K L College of Engineering, Vaddeswaram - 522 502, Guntur Dt., AP

---

## SYNOPSIS

The structure, properties and chemical composition of the weld metal are determined by the fluid flow within the weld pool and the alloying element vaporization from its surface. High temperature surface tension and other thermo physical data are especially important for the analysis of these transport processes. Existing results of physical simulation, mathematical modeling and welding experiments aimed at addressing these issues are reviewed in this paper. Welding parameters like work piece composition and thickness, welding speed and process as well as gravity are correlated to weld bead geometry. Welding models are used to predict microstructure and weld pool shape at different stages.

NOMENCLATURE :  $\eta$  = arc efficiency,  $k$  = heat concentration coefficient,  
GTA = Gas Tungsten Arc; HAZ = Heat Affected Zone 1.

## INTRODUCTION

Welding technology has advanced significantly in the last several decades. Gaps in the understanding of the welding processes have also become apparent as a result of research efforts mainly on the structure and properties of the welds and, to a lesser extent, on the welding processes. During welding, a combination of buoyancy, electromagnetic and surface tension effects leads to vigorous circulation of the weld metal and concomitant convec-

tive mass transfer within the weld pool. The structure, properties and chemical composition of the weld metal are strongly affected by the metal flow in the weld pool and the alloying element loss due to evaporation. Resolution of these issues contributes to improved understanding and control of welding processes.

The uniqueness and the complexity of the various physical phenomena in welding, the presence of plasma close to the weld pool surface and

the scarcity of the thermo-physical data base at temperatures much higher than the melting point, often preclude meaningful comprehensive analysis of welding processes.

A sustained research effort is needed for in-depth investigations of these and other issues related to phenomenological understanding of welding processes and for creation of an appropriate high temperature thermo-physical data base relevant to welding.

## DRIVING FORCES FOR FLUID FLOW

The magnitude and direction of the fluid flow of molten metal in the weld pool can significantly alter the local fluid flow conditions and, consequently, the fusion zone geometry and weld properties. The driving forces for fluid flow in the weld pool fall into two categories: ( 1 ) The volume forcing terms that include the buoyant (thermal/gravity) body forces and electromagnetic body forces and (2) the shear and pressure acting on the weld pool surface due to surface tension gradient and surface curvature. At high welding current, the arc pressure due to plasma arc may influence the fluid flow in the weld pool.

### Buoyancy

Heat flux from the arc generates spatial and temporal density gradients in the metal. Due to the densimetric gradients, mechanical equilibrium in the molten metal is not possible, causing thermally driven flows in the weld puddle, which tend to equalize the temperature everywhere in the puddle.

### Electromagnetic body force

Electric currents and induced magnetic fields can influence fluid flow in the weld pool by way of electromagnetic body force.

### Surface tension

In many welding processes, the primary driving force for fluid flow in the weld pool is the spatial gradient of interfacial tension which results from the temperature variation at the weld pool surface. The intensity and direction of the fluid flow within the weld pool are influenced by the temperature coefficient of surface tension. For pure metals, the temperature coefficient can be estimated. However, most commercial alloys contain small amounts of surface active elements such as oxygen and sulphur. Since these elements are known to affect the temperature coefficient of surface tension significantly, they have major effects on the fluid flow in the weld pool. In order to quantitatively determine their role in establishing weld pool fluid flow, it is necessary to know how the temperature coefficient of

interfacial tension changes with both temperature and composition.

### Vaporization

One of the major problems in the use of a very high power density heat source for metal joining is the loss of volatile alloying elements. The change in the composition is determined by the vaporization rate and the size of the weld pool, the latter being the dominant factor in most cases. The composition changes are most pronounced at low laser powers because all the alloying element loss occurs from a small volume of weld metal.

### Temperature dependent physical properties

The need for a more basic understanding of welding process by computational modeling requires the knowledge of selected thermo-physi-

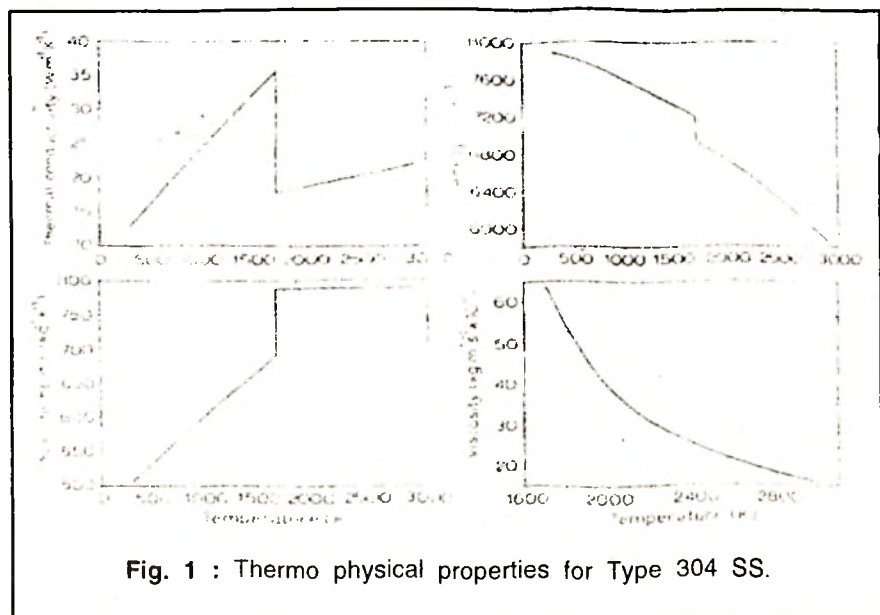


Fig. 1 : Thermo physical properties for Type 304 SS.

cal properties for the range of temperatures of interest. However, detailed information on thermo-physical properties is extremely hard to obtain since there are no experimental data for the thermodynamic and transport properties of most materials at high temperatures. Consequently, most computational modeling efforts to date attempting to study weld pool development have used constant values for selected thermo-physical properties.

Zacharia et al (1) appropriately modified their model to include temperature dependent physical properties. Fig. 1 gives the temperature-dependent thermo-physical properties for Type 304 stainless steel between 300 K and 3000 K. The properties in the solid state may be obtained by extrapolating available experimental data and the properties of the liquid phase may be estimated based on thermodynamic principles.

## Plasma

Although the quality of the weld joint is known to be related to the nature of welding plasma, its role in the welding process is not well understood. Several questions arise in the context of this discussion. Does the plasma affect metal vaporization rate or the interfacial tension? What is its role in affecting the solubility of elements such as nitrogen or oxygen in the weld metal?

## SIMULATION RESULTS AND DISCUSSIONS

The fluid flow in the molten weld pool can significantly affect the puddle geometry and the penetration depth of the pool. This, in turn, affects the temperature gradients in the weld pool and the solidification behavior of the weld. Welding models can be used to estimate the shape of the weld pool as a function

of different driving forces. A convenient way of comparing the shape of weld pools is by plotting the isotherms for different values of driving forces.

The convection patterns and weld penetrations due to individual driving forces were studied separately in order to show the distinct differences among themselves and to help explain those due to the combined driving forces.

## Buoyancy

An example of results of these studies in the case of GTA welding of 304L stainless steel is illustrated in Fig. 2, from the works of Kou and Wang(2). In this example, which shows the front view of the fluid flow pattern, the buoyancy force effect is clearly demonstrated. The flow is from center to boundary.

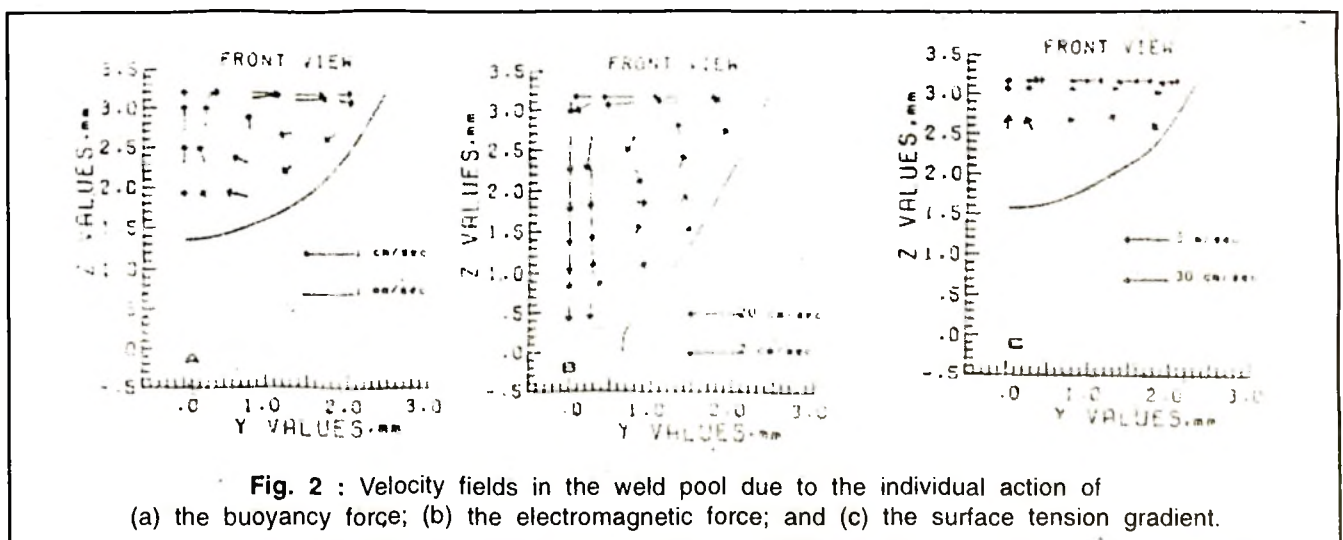


Fig. 2 : Velocity fields in the weld pool due to the individual action of (a) the buoyancy force; (b) the electromagnetic force; and (c) the surface tension gradient.

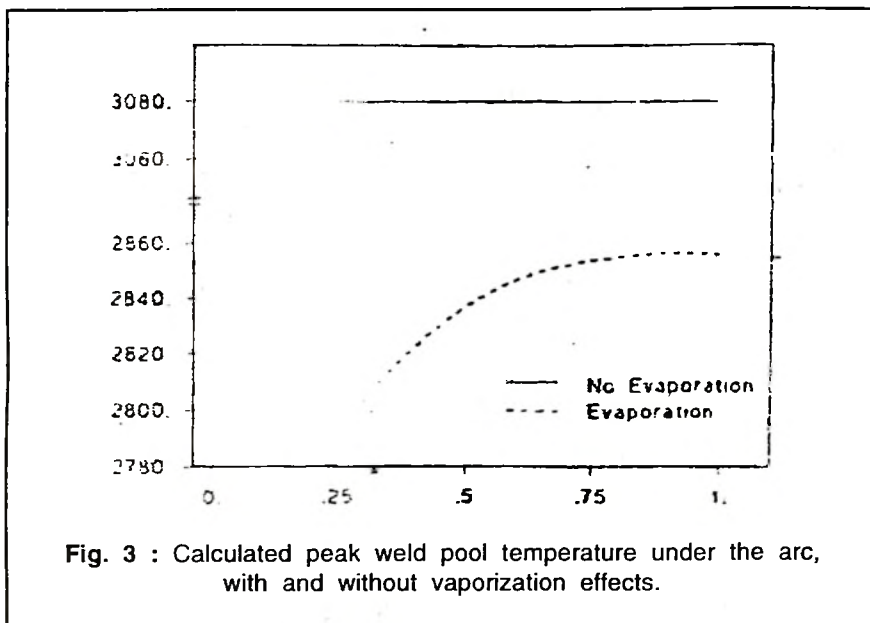


Fig. 3 : Calculated peak weld pool temperature under the arc, with and without vaporization effects.

### Electromagnetic force

Figure 2(b) shows the fluid flow pattern due to the electromagnetic force. As shown, it is in the opposite direction of the buoyancy force driven flow shown in Fig. 2(a). More importantly, the weld pool now penetrates the work piece, indicating the strong influence of electromagnetic force on weld penetration.

### Surface tension

Figure 2(c) shows the surface tension driven flow. The fluid flow pattern is similar to that due to the buoyancy force alone, in that the pool is shallow. Flow at the free surface is from center to boundary and the maximum velocity occurs at the free surface. However, compared to the buoyancy force driven flow, the maximum velocity is much higher, and

the strength of fluid flow below the free surface decays much more rapidly.

### Vaporization

Although it has been recognized that metal vaporizes during welding, the effect of vaporization on fluid flow has not been studied in detail. An indication of how weld pool vaporization affects peak weld pool temperature under the arc is given in Fig. 3. It is seen in this figure, due to Zacharia and David(3), that when weld pool vaporization is taken into account, the peak weld pool temperature increases monotonically with time until a maximum value which is limited by the vaporization heat flux, is reached. On the other hand, the results indicate that in the absence of vaporization the peak weld pool quickly reaches the boiling temperature.

## CORRELATION BETWEEN WELDING PARAMETERS AND WELD BEAD GEOMETRY

Within the welding context the principal objective of process research is to relate the welding parameters to the structure and properties of the welds produced. This helps to define the optimal welding conditions and ultimately to devise the means of accomplishing these through automation, process control and robotization.

### Composition

The effect of workpiece composition is illustrated in Fig. 4 in the case of welding of Aluminum base alloys, from the works of Marya and Kim(4). The isotherms for two different materials are plotted in the x-y plane of the plate being welded. The significance of composition is very apparent.

### Thickness

Gray(5) investigated the effect of increase in the plate thickness. The much higher efficiency of cooling of thick plates has the effect of reducing the size of the weld deposit as shown in Fig.5.

### Welding speed

The effect of the welding speed on the temperature distribution was studied by Sharir et al (6). The tem-

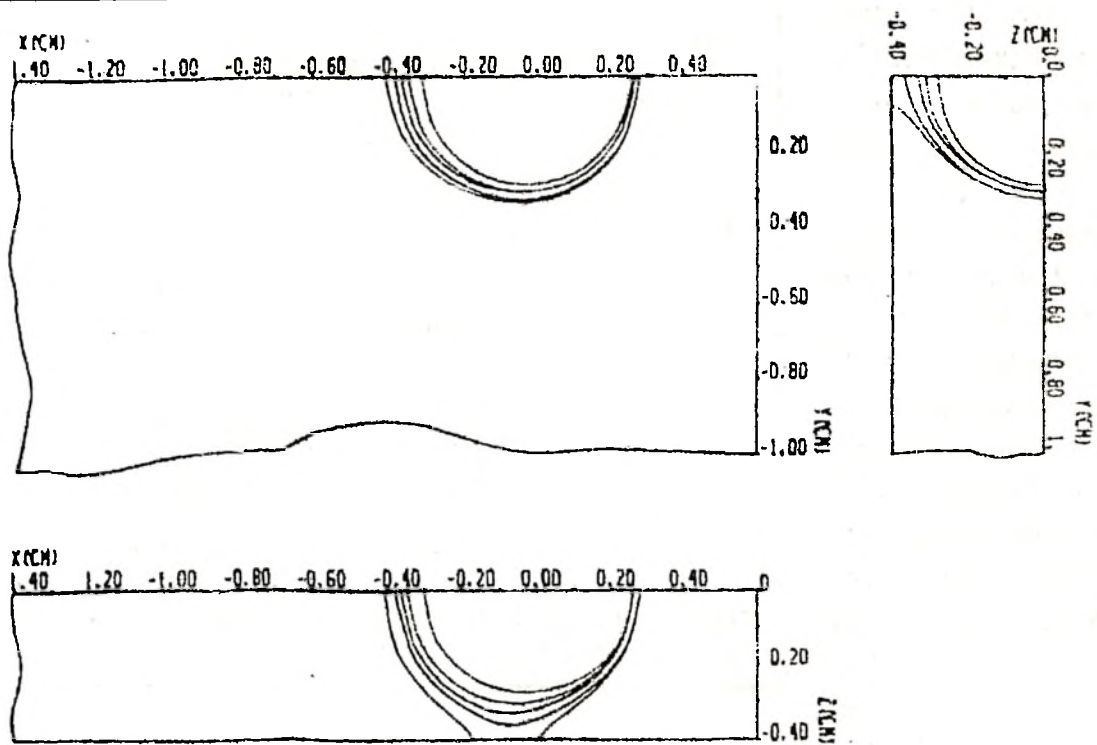


**Fig. 4 :** Comparison of liquidus isotherms of different alloys. From center to exterior represents the fusion zone of alloy 1050A, 6061,7020,2017A and 5083 respectively.

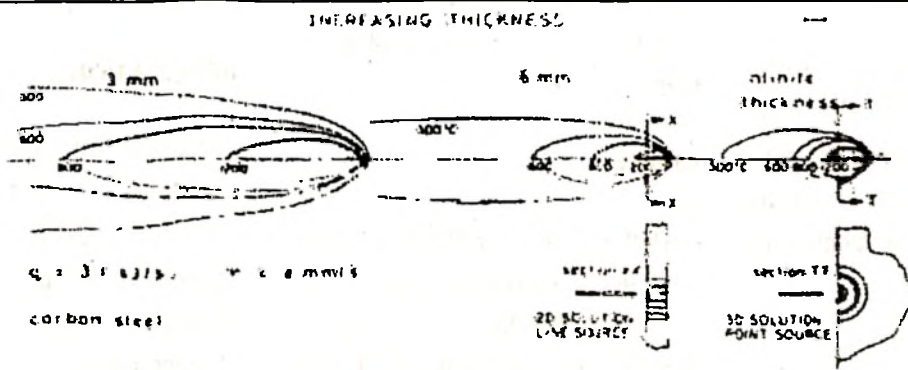


**Fig. 5 :** Effect of changes in steel plate thickness on isotherm shape.

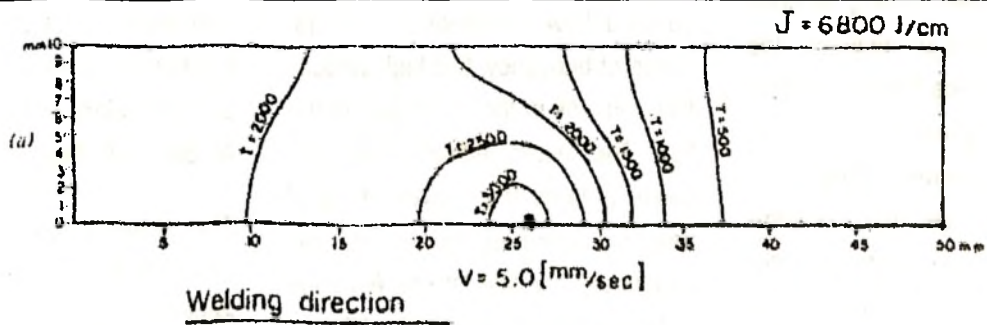


**Fig. 6 :** Isotherms during steady state at different welding speeds; (a) -5.0 mm/s; (b) -8.33 mm/s; (c) -1 1.67 mm/s.

perature distributions at the steady state at different welding speeds is shown in Fig.6. As can be seen, there is a gradual change in the shape of the pool from an elliptic to a tear drop shape with the increase in the speed of welding. This explains the changes in the orientation of the grains in the fusion zone with the increase in welding speed. The orientation of the grains change from almost parallel to the welding direction at a slow welding speed to nearly perpendicular to the welding direction at a high speed. It should be emphasized that the microstructure in the fusion zone is determined by the shape of the solidification front, that is the shape of the trailing end of the liquid pool.

The effect of increasing welding speed is to concentrate the heat closer to the source and this has important implications on solidification structure, thermal gradients and turbulence in the melt.

### Welding process

Depending on the welding technology and computation methods, the arc efficiency varies from the lowest 20% to the highest 90%. Taking these extreme values, Marya and Kim(4) demonstrated that the computed weld pool would show sometimes non-melted or fully penetrated weld in place of a partially penetrated experimental weld (Fig.7).

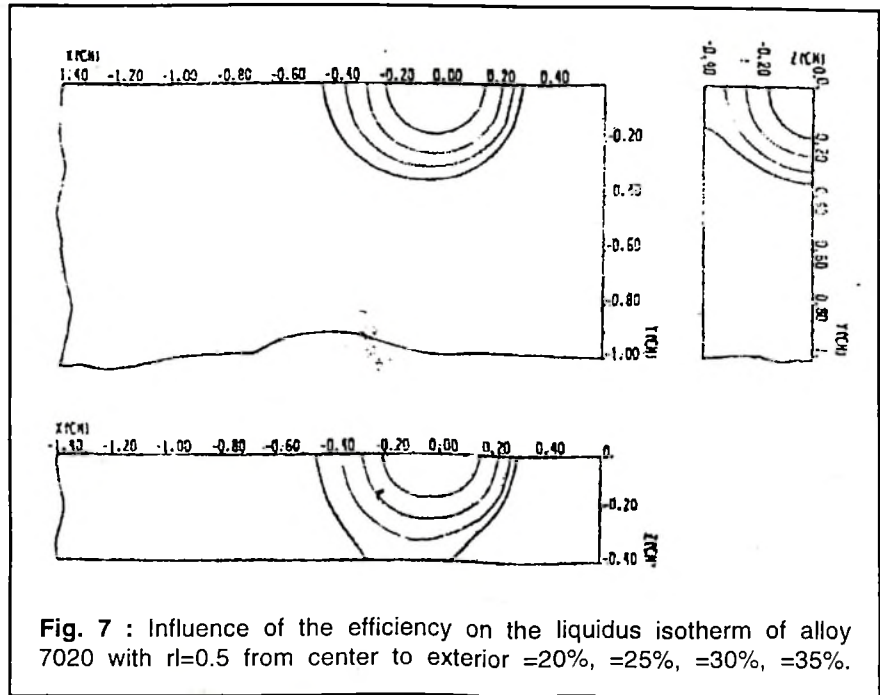


Fig. 7 : Influence of the efficiency on the liquidus isotherm of alloy 7020 with  $\eta=0.5$  from center to exterior =20%, =25%, =30%, =35%.

The above results may probably be extended to determine whether a particular welding process is suitable to weld a work piece of specified thickness.

### Gravity

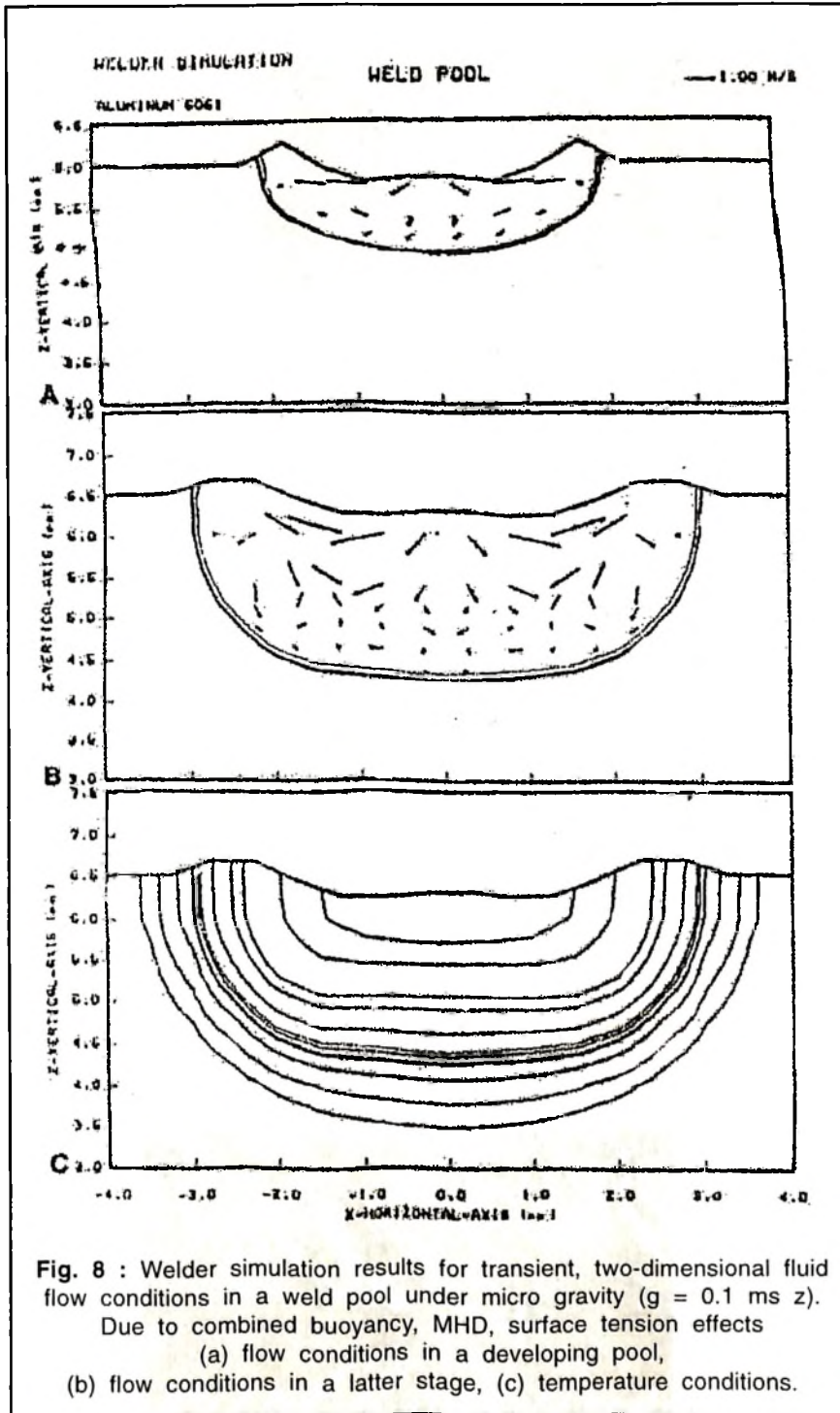
Zacharia et al (7) simulated natural and forced convection due to the combined driving forces in micro gravity environment Fig. 8. Marangoni effect drives a radially outward flow. However, in the absence of buoyancy, this high velocity flow remains in the top region of the flow. The results indicate that there exists a fairly thick layer of liquid near the bottom of the pool that experiences very little mixing. Also, the weld pool has a significantly different shape, as can be seen from the isotherms within the weld pool.

However, outside the pool, the conduction effect results in concentric temperature contour.

### APPLICATIONS

Computational modeling is a valuable tool in understanding the various physical phenomena as demonstrated in the previous sections. However, to realize the full potential of computational modeling, it should be possible to simulate more general and practical problems, such as prediction of microstructure, weld pool boundary and weld pool shape at different stages of welding.

The grain structure of fusion and heat-affected zones of a weld are dependent to a large extent on the thermal history of the material during welding. The mechanical properties



of the weld are dependent, among other things, on the microstructure of the weld, that is, of the fusion zone and of the heat affected zone, HAZ. From the calculated temperature

distribution and shape of liquid pool the grain size in the HAZ and grain orientation in the fusion zone can be explained. The thermal stresses during welding and the residual

stresses developed also depend on thermal history. A proper control of the welding process therefore requires the knowledge of the temperature distribution. Employing the model for calculating the thermal history, the optimum welding parameters can be chosen to obtain the best properties of the welded material within the limitations prevailing in the process considered.

### Microstructure

Kou and Kanevsky(8) studied the weld microstructure near the weld centerline and the fusion line (Fig.9). As can be seen in Figs. 9(a) and (b), the cell spacing of the solidification structure is finer near the weld center line due to the higher cooling rate and coarser near the fusion line due to lower cooling rate.

Finally, Fig. 9(c) shows the higher magnification of Fig. 9(b) at a position near the fusion line but outside the fusion zone. Calculation shows that the peak temperature experienced by the work piece at this position was above the solidus temperature and below the liquidus temperature, thus indicating that the eutectic material here melted during welding. As can be seen in Fig. 9(c), the welding of the structure by the eutectic material (which is sometimes responsible for hot cracking in aluminum alloy) is clearly visible.

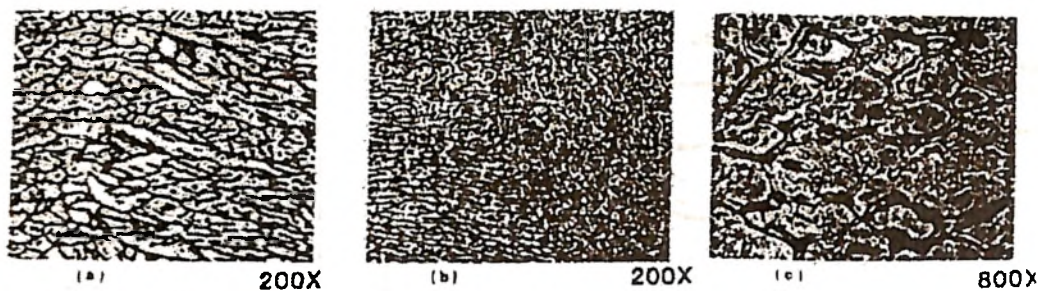


**Fig. 9 :** The weld microstructure transverse to the welding direction of a thin 6061 aluminum plate; (a) coarse cell spacings near the fusion line; (b) fine cell spacings near the weld center line and (c) wetting of the structure by the eutectic material just outside the fusion zone.

### Weld pool boundary

S.Kou and Kanevsky(8) investigated heat flow and solidification during the welding of thin 6061 aluminum plates. Autogenous, full penetration welds were made using GTA welding. In order to check the calculated temperature distribution, the calculated liquidus isotherm is superimposed on the weld microstructure in Fig. 10. By doing this the calculated pool boundary, i.e., the liquidus isotherm can be compared directly with the weld microstructure. As can be seen, the width of the calculated pool boundary is very close to the width of the fusion zone.

### Weld pool shape at different stages

Sharir et al (6) calculated the temperature distribution at a welding rate of 1.67 mm/s at different stages (Fig.11 ). In this figure, the isotherm are indicated for three positions of the arc (the black dot represents the

center of the arc), that is, at the initial, intermediate and final stage of the welding. The boundary of the liquid pool is outlined by the isotherm of 3000 °C. The liquid pool and the temperature distribution around it, as shown in Fig. 11(b), are representative of the steady state stage of the welding. It should be emphasized that the calculation started when the whole specimen was at room temperature (25°C). The shape of the liquid pool is a

result of the calculation, and not an assumed initial condition. It evolves from an initial state, Fig.11(a), through a steady state (Fig. 11b) to its final shape (Fig. 11c). Calculation beyond the point indicated in Fig.12(c), results in a continuous increase of the width of the liquid pool. This corresponds to the actual run-out of the liquid metal, observed experimentally when the welding arc continues to move up

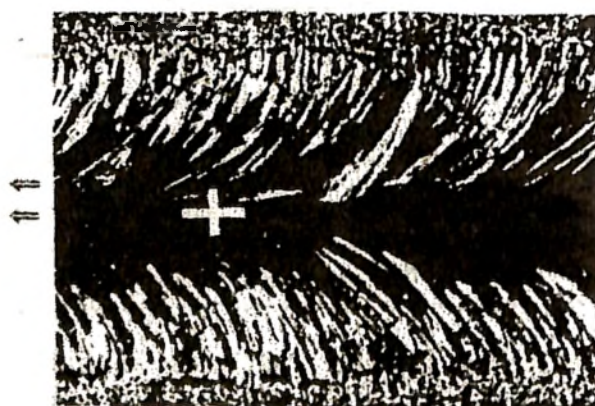


**Fig. 10 :** The weld macrostructure of a thin plate of 6061 aluminum (x10). The broken curve is the calculated weld pool boundary during welding.

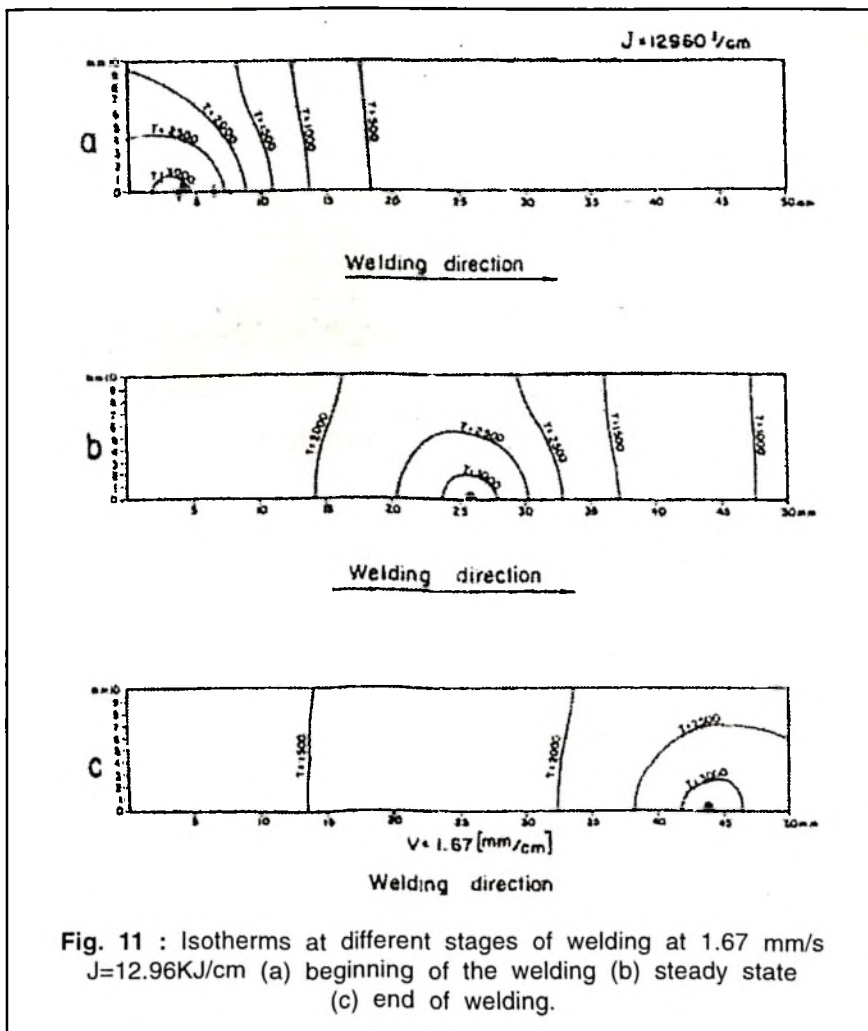


Fig. 11 : Isotherms at different stages of welding at 1.67 mm/s  $J=12.96\text{KJ/cm}$  (a) beginning of the welding (b) steady state (c) end of welding.

to the edge of the specimen. The calculated width of the liquid pool agrees with the experimentally observed width of about 5mm of the fusion zone.

### CONCLUSIONS

The general survey of the published literature on the simulation of fluid flow in weld pools invariably leads to the conclusion that the fit between computed and experimental results is good. However, a deeper survey and close examination of the

published documents show that the fit is always obtained by choosing appropriate numerical values of the effective heat input or by adjusting the energy distribution in welding arc. This is a serious handicap for different models supposed to give prior evaluation of weld thermal cycles. Yet, it is qualitatively possible to appreciate how different welding parameters would affect the temperature distribution, once the model has been calibrated to some experimental values.

### REFERENCES

1. Zacharia, T., David, S.A., Vitek, J. M. and Kraus, H G. 1991, Metallurgical Transactions B, Volume 22B, 243.
2. Kou, S. and Wang, Y. H. 1986, Welding Research Supplement, 63-5
3. Zacharia, T., David, S.A., Vitek, J.M. and Kraus, H.G. 1993, Mathematical modeling of weld phenomena, Ed. Cerjak, H. and Easterling, K. E., The Institute of Materials, London.
4. Marya, S.K and Kim, J.I. 1985, State of the art document, IIW Annual Assembly.
5. Gray, T.G. et.al. 1992, Newnes-Butterworth, Ed. Easterling, K. Second Edition, Butterworth Heinemann, Oxford.
6. Sharir, Y., Grill, A., and Peileg, J. 1980, Metallurgical Transactions B., Volume 11 B, p257.
7. Zacharia, T., Eraslan, A.H. and Aidun, D.K. 1988, Welding Research Supplement.
8. Kou, S. and Kanevsky, T. 1982, ASM, Ohio.